JOURNAL OF MATERIALS SCIENCE 27 (1992) 908–912

Indentation technique for evaluation of hot hardness and creep of SS 316 end-plug welds of nuclear fuel pins

T. R. G. KUTTY, C. GANGULY
Radiometallurgy Division, Bhabha Atomic Research Centre, Trombay, Bombay 400 085, India

The high-temperature mechanical properties of SS 316 end-plug welds of nuclear fuel pins were studied using a hot hardness tester. The hardness was measured as a function of temperature on the base metal, weld pool and heat-affected zone from ambient temperature to 1273 K. Hardness was also measured as a function of dwell time from 873 to 1173 K to evaluate the activation energy for creep. The activation energy of the weld pool was found to be higher than that of the base metal. The indentation technique is very suitable for the evaluation of creep properties of very small components.

1. Introduction

The indentation technique is a highly attractive tool for evaluation of the hot hardness and creep properties of small components. The main advantage of this technique is that it gives reliable information on mechanical properties within a short time. Indentation tests can be successfully employed for evaluating the creep behaviour of the end-plug welds of nuclear fuel pins.

Stainless steel (SS) type AISI 316 is being widely used as the cladding material for nuclear fuel pins for fast reactors. The tungsten inert gas (TIG) welded SS 316 end-plugs display a complex and non-uniform structure, namely columnar grains, additional phases and contamination due to impurities. In the present investigation the hot hardness and activation energy for creep of the weld region and base metal of SS 316 end-plug welds have been evaluated by the indentation technique.

2. Principles

The temperature dependence of hardness has been investigated by many authors [1–3] and the following relation is widely used:

$$H = A \exp(-BT) \quad (1)$$

where H is the hardness, T is the temperature (K), A is the intrinsic hardness (i.e. the value of hardness at $T = 0$ K) and B is the softening coefficient.

A plot of $\log H$ versus T yields two straight lines which intersect at around $0.5T_m$ where T_m is the melting point. The temperature corresponding to the change in slope of the $\log H$ versus T plot is called the transition temperature. Creep deformation is significant only above the transition temperature.

Indentation creep properties at any particular temperature are estimated by measuring the hardness as a function of time. When $\log H$ is plotted against $\log t$ (where t is the dwell time of indentation) a series of parallel straight lines is obtained for different temperatures. Bowden and Tabor [4] have given the following relation between hardness and time for constant load:

$$H^{-(n+0.5)} = A[\exp(-Q/RT)]t \quad (2)$$

where t is the time, Q is the activation energy and A and n are constants.

The activation energy is calculated from the relative displacement of parallel lines corresponding to different temperatures using the relation [5–6]

$$Q = R\frac{\ln t_1 - \ln t_2}{(1/T_1) - (1/T_2)} \quad (3)$$

where t_1 and t_2 are the times to yield a constant hardness at temperatures T_1 and T_2.

3. Experimental procedure

The chemical composition of stainless steel type AISI 316 used in this study is given in Table I. Dummy pins were fabricated by TIG welding of end-plugs (Table II) with a cladding tube of outer diameter 5.1 mm and

TABLE I Composition of stainless steel type AISI 316 (wt %)

C	Cr	Ni	Mo	Mn	Si	N	Fe
0.05	17	13	2	2	0.6	0.06	Bal.

TABLE II Parameters used for end-plug welding

Initial current	6A
Weld current	13 A
Arc voltage	17.5 V
Arc gap	0.5 mm
Torch gas flow	0.11 $m^3 h^{-1}$
Weld time	7 s
Annealing time	4 s

0022–2461

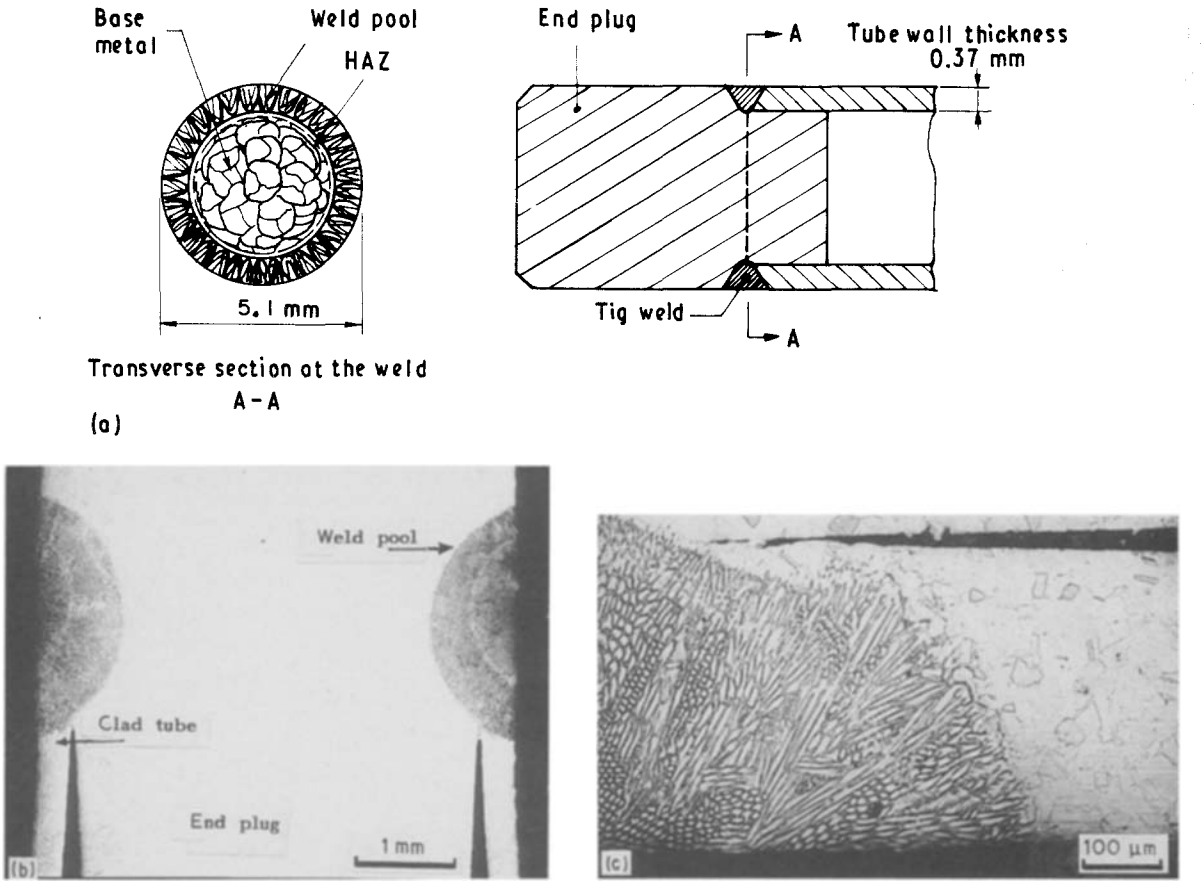

Figure 1 (a) Schematic view of a fuel end-plug showing the weld region; (b) macrophotograph of the weld region; (c) typical microstructure of the weld region.

wall thickness 0.37 mm as shown schematically in Fig. 1a. The weld joints were subjected to helium leak testing and X-ray radiography. Only accepted welds were taken for hot hardness measurements. Samples were cut from the fuel pin and mounted, ground, polished and etched electrolytically using 10% oxalic acid. Typical microstructures of the weld are shown in Fig. 1b and c. The weld penetration in all cases was more than 110% of the wall thickness. The microstructure of the weld pool consists of columnar grains surrounded by a small region of heat-affected zone (HAZ) having a width of $\sim 50\,\mu m$. The amount of δ-phase present in the weld pool (WP) is 2 to 3% [7].

The room-temperature microhardness values of WP, HAZ and base metal using 100 g load are shown in Fig. 2.

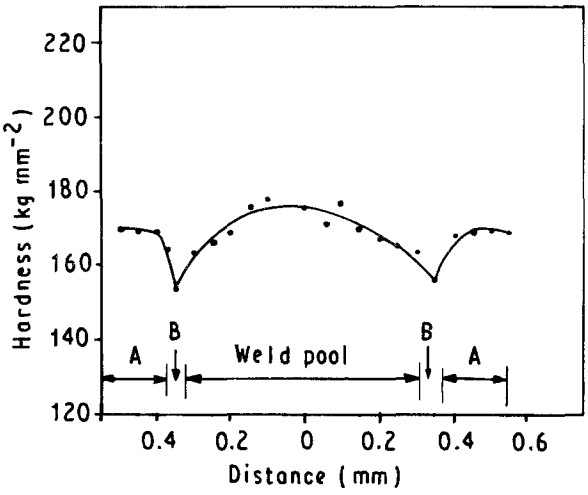

Figure 2 Room-temperature microhardness values of weld pool, HAZ (B) and base metal (A) plotted against the distance from the centre of the weld pool.

3.1. Hot hardness

The hot hardness measurements were carried out from ambient temperature to 1273 K at every 100 K interval using a Nikon Model-QM unit fitted with a micro-Vickers indentor. The specimen was mounted inside the furnace, keeping the measurement surface perpendicular to the microscope axis. The hardness data were evaluated on WP, HAZ and base metal. The dwell time in all measurements was 5 s. The indentation diagonals were measured at × 500 magnification with an accuracy of 0.1 µm. Four readings were taken at each temperature and their average values were recorded.

3.2. Indentation creep

Indentation creep measurements were carried out at 873 to 1173 K at intervals of 100 K. The hardness at each temperature, as a function of dwell time corresponding to 1, 5, 10, 50, 100, 200 and 1000 s, was measured. Four readings were taken for each dwell time and their average value was recorded. Indentation creep studies could not be carried out on the HAZ because of its small area.

4. Results

The hardness versus temperature plots for WP, HAZ and base metal are shown in Fig. 3 and were found to obey the relation

$$H = A\exp(-BT)$$

The values of A and B determined for all three zones are given in Table III. The hardness was found to decrease gradually up to the transition point which occurs at around 973 K. Above the transition point the hardness decreased rapidly with temperature. The hardness of the WP and HAZ were highest and lowest, respectively, up to the transition point.

The hardness versus time plots for WP and base metal at various temperatures are shown in Figs 4 and 5. The activation energy for creep was estimated from these plots using Equation 3. The hardness versus

TABLE III Values of constants of Equation 1 for the low-temperature part of $\log H$ versus T plot

	A (kg mm^{-2})	B (K^{-1})
Weld pool	187	− 0.00082
Base metal	181	− 0.00081
HAZ	177	− 0.00087

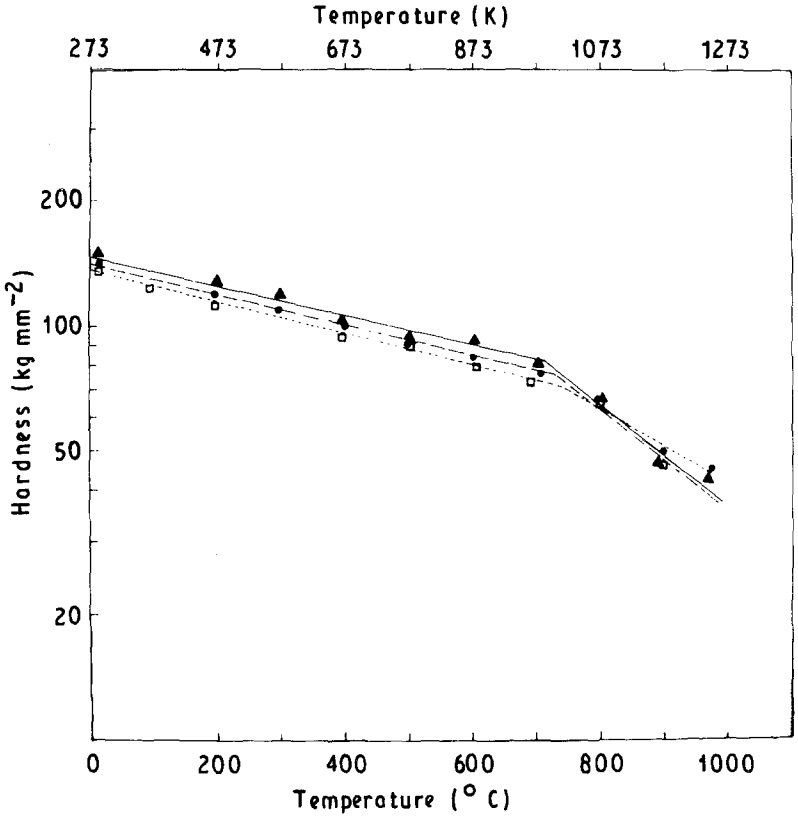

Figure 3 Plots of log (hardness) versus temperature for (▲) WP, (□) HAZ and (●) base metal.

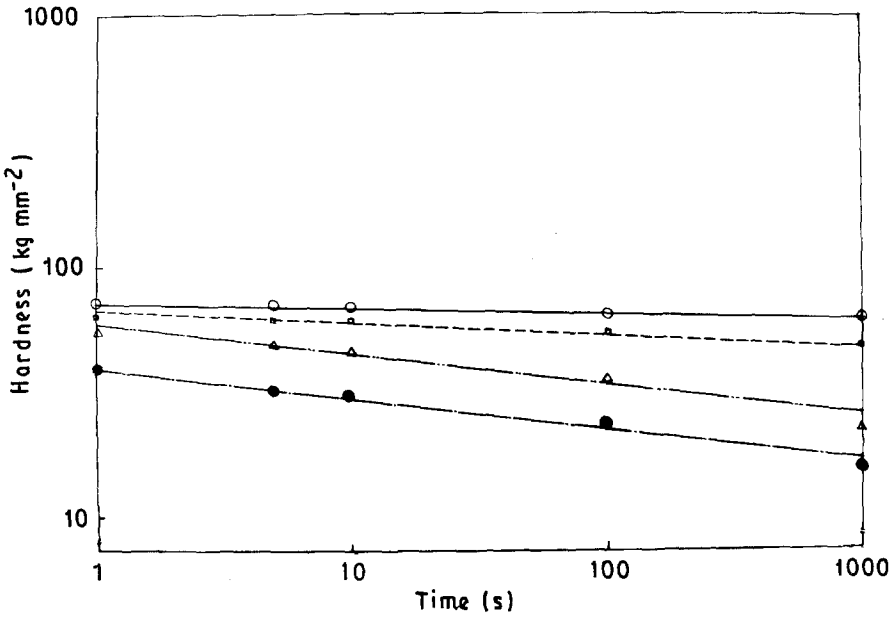

Figure 4 Effect of dwell time on hardness at various temperatures for the weld pool: (○) 873 K, (□) 973 K, (△) 1073 K, (●) 1173 K.

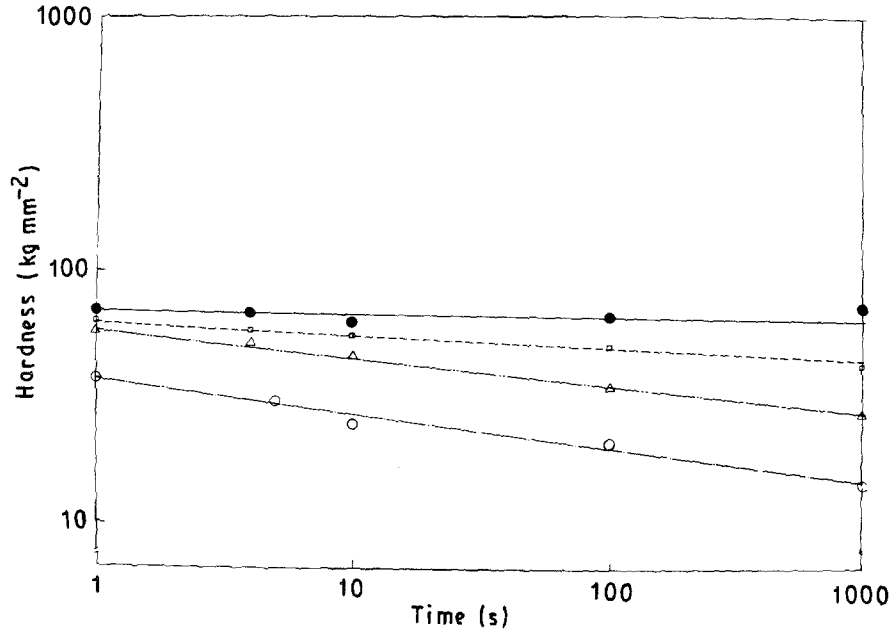

Figure 5 Effect of dwell time on hardness for base metal at different temperatures: (●) 873 K, (□) 973 K, (△) 1073 K, (○) 1173 K.

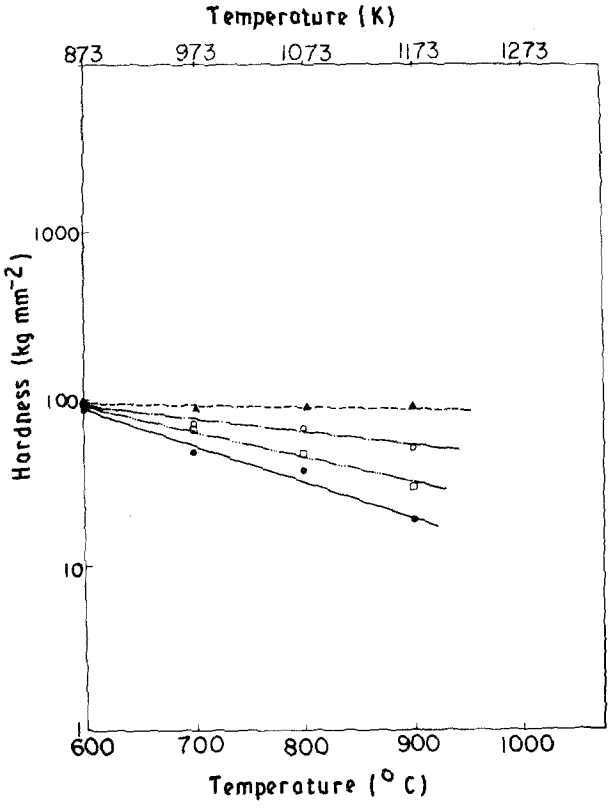

Figure 6 Plot of log (hardness) versus temperature at the weld pool for different dwell times: (▲) 1 s, (○) 10 s, (□) 100 s, (●) 1000 s.

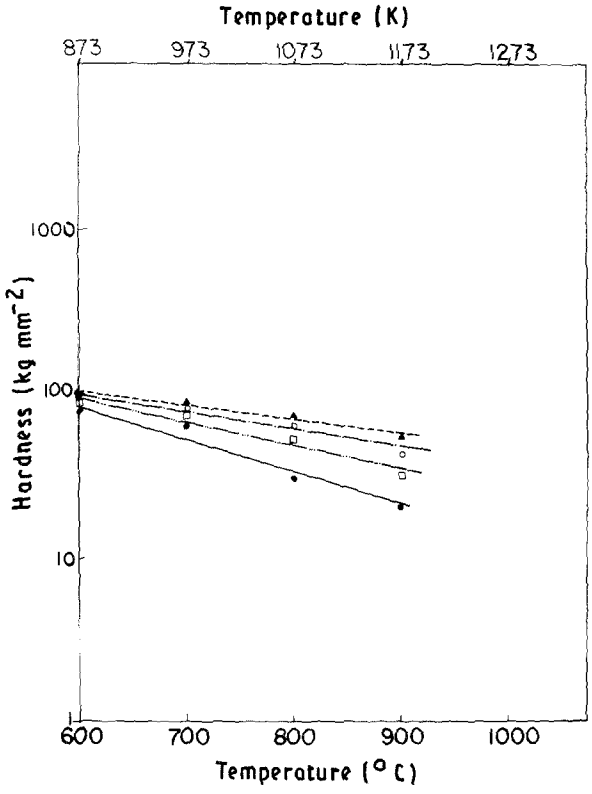

Figure 7 Log (hardness) versus temperature plot for different dwell times at the base metal: (▲) 1s, (○) 10 s, (□) 100 s, (●) 1000 s.

temperature plots at and above 873 K for various dwell times are given in Figs 6 and 7.

The activation energy for creep of base metal and WP were found to be 347 ± 12 and 435 ± 12 kJ mol^{-1}, respectively. Hence the weld pool is more creep-resistant than the base metal since the activation energy for creep is higher for the former.

5. Discussion

The thermal creep properties of SS 316 base materials and welds have been studied by many authors [8–13]. The activation energy for creep estimated in this study is found to be higher than the diffusional activation energy which for stainless steel is 280 kJ mol^{-1} [14]. A mechanism based on the climb of edge dislocations or the motion of jogged screw dislocations requires an activation energy which should be equal to the diffusional activation energy. Similarly models based on Nabarro–Herring or Coble creep require an activation energy equal to or less than the diffusional activation energy [15, 16]. Since the activation energy in the

weld pool of SS 316 is higher by about 50% than the reported value of diffusional activation energy, the above mechanisms are not the rate-controlling mechanism.

The higher activation energy for creep obtained in this study may be attributed to the mechanism of unpinning of attractive junctions suggested by many authors [17–20]. According to this model, at low temperatures an attractive junction is broken only by means of glide dislocation bowing around the junction. At higher temperatures enough thermal energy is available to unpin the junctions in preference to bowing. A dislocation link length is thus released and is free to glide until it meets a second forest dislocation that produces a strong enough attractive junction. The dislocation waits here until a successful thermal fluctuation assists the applied stress in bringing together the two threefold nodes separating the junction, thereby releasing the dislocation segment, and this process goes on. The activation energy for this mechanism is a function of stacking fault energy.

6. Conclusion

The indentation technique utilized for the evaluation of hot hardness and creep properties of SS 316 end-plug welds of nuclear fuel pins reveals that the weld pool is more creep-resistant than the base metal. The mechanism proposed for the creep phenomenon is the unpinning of attractive junctions.

Acknowledgements

The authors would like to acknowledge Professor D. H. Sastry, Department of Metallurgy, Indian Institute of Science, Bangalore for his valuable suggestions. They also wish to record their sincere thanks to Messrs S. Chatterji and S. Ananatharaman for useful discussions.

References

1. J. H. WESTBROOK, *Trans. ASM* **45** (1953) 220.
2. E. R. PETTY, *Metallurgia* **56** (1957) 231.
3. D. TABOR, *Rev. Phys. Technol.* **1** (1970) 145.
4. F. P. BOWDEN and D. TABOR, "The Friction and Lubrication of Solids", Part 2 (Oxford University Press, London, 1964) p. 338.
5. U. ROY and D. GLASSCO, *J. Less-Common Metals* **29** (1972) 229.
6. T. O. MULHEARN and D. TABOR, *J. Inst. Metals* **89** (1960–61) 7.
7. G. L. GOSWAMI, J. K. GHOSH, V. D. PANDEY and P. R. ROY, *J. Machine Bldg Indy* **20** (10) (1981) 476.
8. P. MARSHALL, "Austenitic Stainless Steel: Microstructure and Properties (Elsevier Applied Science, Essex, UK, 1984) p. 233.
9. H. J. KESTENBACH, W. KRAUSE and T. L. SILVERIA, *Acta Metall.* **26** (1978) 661.
10. O. K. CHOPRA and K. NATESAN, *Met. Trans.* **8A** (1977) 633.
11. G. W. GREENWOOD, H. JONES and T. SRITHARAN, *Phil. Mag.* **41** (1980) 871.
12. R. G. THOMAS, *Welding J.* **58** (1978) 81s.
13. B. A. SENIOR, *J. Mater. Sci.* **25** (1990) 45.
14. H. J. FROST and M. F. ASHBY, "Deformation Mechanism Maps" (Pergamon, Oxford, 1982) p. 62.
15. R. W. EVANS and B. WILSHIRE, "Creep of Metals and Alloys" (Institute of Metals, London, 1985) p. 104.
16. O. D. SHERBY and P. M. BURKE, *Progr. Mater. Sci.* **13** (1968) 381.
17. G. SAADA, *Acta Metall.* **8** (1960) 200.
18. *Idem, ibid.* **8** (1960) 841.
19. D. H. SASTRY, M. J. LUTON and J. J. JONES, *Phil. Mag.* **30** (1974) 115.
20. W. CARRINGTON, K. F. HALE and D. McLEAN, *Proc. R. Soc.* **A259** (1961) 203.

Received 25 October 1990
and accepted 25 March 1991